Age of emplacement and basement character of the Cache Creek terrane as constrained by new isotopic and geochemical data[1]

MITCHELL G. MIHALYNUK AND MOIRA T. SMITH

*Mapping and Resource Evaluation, British Columbia Geological Survey Branch, 553 Superior Street, Victoria, B.C.,
Canada V8V 1X4*

JANET E. GABITES AND DITA RUNKLE

*Department of Geological Sciences, The University of British Columbia, 6339 Stores Road, Vancouver, B.C.,
Canada V6T 2B4*

AND

DAVID LEFEBURE

Economic Geology, British Columbia Geological Survey Branch, 553 Superior Street, Victoria, B.C., Canada V8V 1X4

New U−Pb and Rb−Sr isotopic and major and trace element geochemical data are reported for Late Triassic to Eocene granite bodies that intrude the Cache Creek and Stikine terranes in the Atlin−Bennett area of northwestern British Columbia. The U−Pb isotopic age data help constrain closure of the Cache Creek ocean and obduction of the Cache Creek terrane to before 172 Ma (Middle Jurassic). Low $^{87}Sr/^{86}Sr$ initial ratios (0.7037−0.7046) and lack of evidence for inheritance in zircons suggest that rocks underlying the Cache Creek terrane are largely primitive in nature, with derivation of intrusive rocks predominantly from unevolved sources.

A genetic link between Late Triassic granitic plutons and Stuhini arc volcanics of Stikinia is supported by trace and rare-earth element data which indicate generation of magma in a volcanic-arc setting. Geochemical patterns for postaccretion Middle Jurassic and Late Cretaceous to early Tertiary age plutons are similar to those of the Late Triassic, indicating that Middle Jurassic and younger plutons could be derived from the same source area as the Late Triassic plutons.

These data do not support recent theories proposing that the Cache Creek and Stikine terranes are klippe overlying a thick section of deformed, Proterozoic and lower Paleozoic continental-margin strata and attenuated cratonal basement. Rather, they are consistent with models in which remnants of Cache Creek ocean basin are placed over the Stikine arc in the Early to Middle Jurassic. Both terranes in turn overlie mainly late Paleozoic to early Mesozoic juvenile crustal material or the upper mantle.

Nous présentons de nouvelles données géochimiques fournies par les analyses des isotopes U−Pb et Rb−Sr, des éléments majeurs et des éléments traces des corps granitiques, datant du Trias tardif à l'Éocène, qui recoupent les terranes de Cache Creek et de Stikine de la région d'Atlin−Bennett, dans le nord-ouest de la Colombie-Britannique. Les âges fournis par les isotopes U−Pb servent à définir une limite temporelle, antérieure à 172 Ma (Jurassique moyen), pour les évènements de fermeture de l'océan Cache Creek et de l'obduction du terrane de Cache Creek. Les faibles rapports $^{87}Sr/^{86}Sr$ initiaux (0,7037−0,7046) et l'absence d'indication de zircons hérités suggèrent que les roches sous-jacentes au terrane de Cache Creek sont surtout d'origine primaire; elles proviendraient principalement de magmas non différenciés.

Les résultats des analyses des éléments traces et des terres rares, lesquels indiquent une origine magmatique dans un contexte d'arc volcanique, renforcent l'interprétation d'une parenté pétrogénétique entre les plutons granitiques du Trias tardif et les volcanites de l'arc de Stuhini de la Stikinie. Les distributions géochimiques pour les plutons postaccrétionnaires, d'âge jurassique moyen et crétacé tardif à tertiaire précoce, indiquent que les plutons du Jurassique moyen ou plus jeunes et les plutons du Trias tardif, pourraient provenir d'un lieu magmatique commun.

Ces résultats ne plaident pas en faveur des récentes théories qui proposent que les terranes de Cache Creek et de Stikine représentent une klippe superposée sur une puissante coupe de strates de marge continentale, déformées, d'âge protérozoïque et paléozoïque inférieur, et sur un socle cratonique atténué. Les données s'harmonisent plus avantageusement avec les modèles suggérant que les vestiges du bassin de l'océan Cache Creek furent transportés au-dessus de l'arc de Stikine durant le Jurassique précoce à moyen. Les deux terranes chevauchent à leur tour, principalement, des roches crustales jeunes de la fin du Paléozoïque à début du Mésozoïque, ou des roches du manteau supérieur.

[Traduit par la rédaction]

Introduction

Isotopic and lithologic similarities between the Yukon−Tanana and Nisling terranes and other deformed continental-margin rocks (e.g., Mortensen 1992; Wheeler and McFeely 1987) indicate that these metamorphic rocks envelop the northern termination of the exotic, oceanic Cache Creek terrane and the Stikine arc (Fig. 1a). Sm−Nd and detrital zircon studies indicate that the metamorphic belt is of continental affinity (e.g., Samson *et al.* 1990; Gehrels *et al.* 1991b; Jackson *et al.* 1991; Mortensen 1992; and references therein). If this is correct, then it is necessary to explain how the Stikine and Cache Creek terranes come to lie inboard of the western extension of these packages of continental-margin rocks. This geometry places severe constraints on models for the tectonic evolution of the northern Canadian Cordillera.

To explain the distribution of Stikine arc rocks and Cache Creek oceanic rocks enveloped by "Yukon Crystalline terrane" continental-margin rocks, Tempelman-Kluit (1979) suggested a simple continental rift and collapsed ocean basin
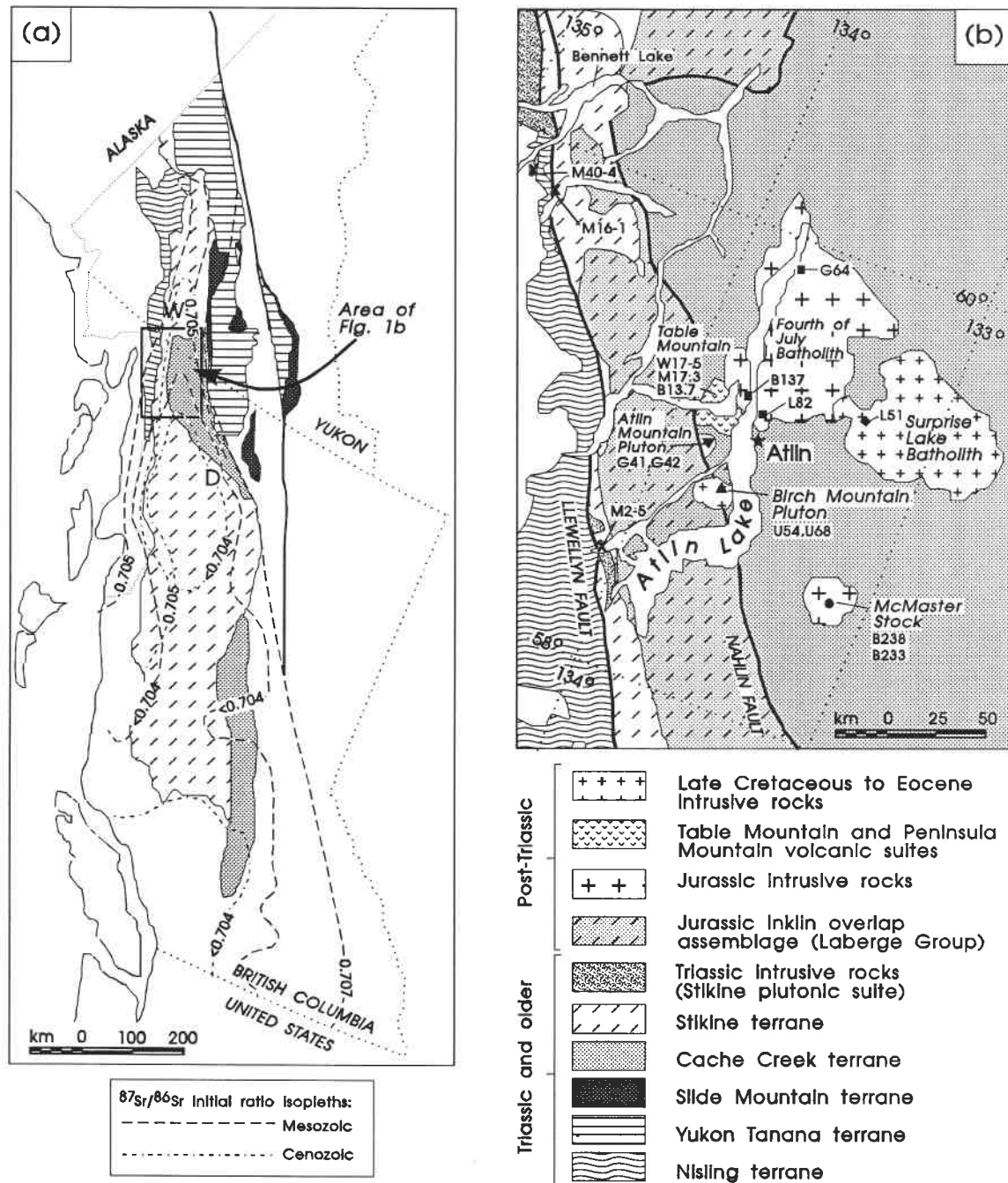
FIG. 1. (a) Distribution of terranes (adapted from Wheeler and McFeely 1987; Hansen 1990; and Mortensen 1992). W and D show localities of the towns of Whitehorse and Dease Lake, respectively. $^{87}Sr/^{86}Sr$ initial ratio isopleths are modified after Armstrong (1988). (b) Generalized geology of the Bennett–Atlin area, showing the distribution of granitoid bodies that intrude the Cache Creek terrane location of samples. ▲, Birch Mountain pluton; ▼, Atlin Mountain pluton; ■, Fourth of July batholith; ●, McMaster stock; ♦, Surprise Lake batholith; ×, Stikine plutonic suite.

model (Fig. 2a). In his model, a portion of the continental margin rifted away from the craton to form the Anvil ocean (Slide Mountain and Cache Creek terranes). Subsequent closure and subduction of this ocean basin formed the Stikine arc. Complete closure of the basin culminated in obduction of part of the oceanic crust and mantle and a reunion of the Yukon Crystalline terrane with the continental margin.

Slide Mountain oceanic rocks, which are of North American affinity, were later recognized to be distinct from Cache Creek rocks of Tethyan affinity (Monger and Ross 1971; Monger

1977; Monger and Price 1979). At the same time, paleomagnetic evidence appeared to require thousands of kilometres of northward translation of the western Cordillera to accommodate aberrant paleopoles (e.g., Irving *et al.* 1985). Such observations were explained by the terrane hypothesis which stated that crustal fragments from apparently widely varying paleogeographic settings were amalgamated during mainly northeastward transport (Coney *et al.* 1980; Monger *et al.* 1982) (Fig. 2b). However, a subsequent reinterpretation of the paleomagnetic data (e.g., Butler *et al.* 1989; Irving and
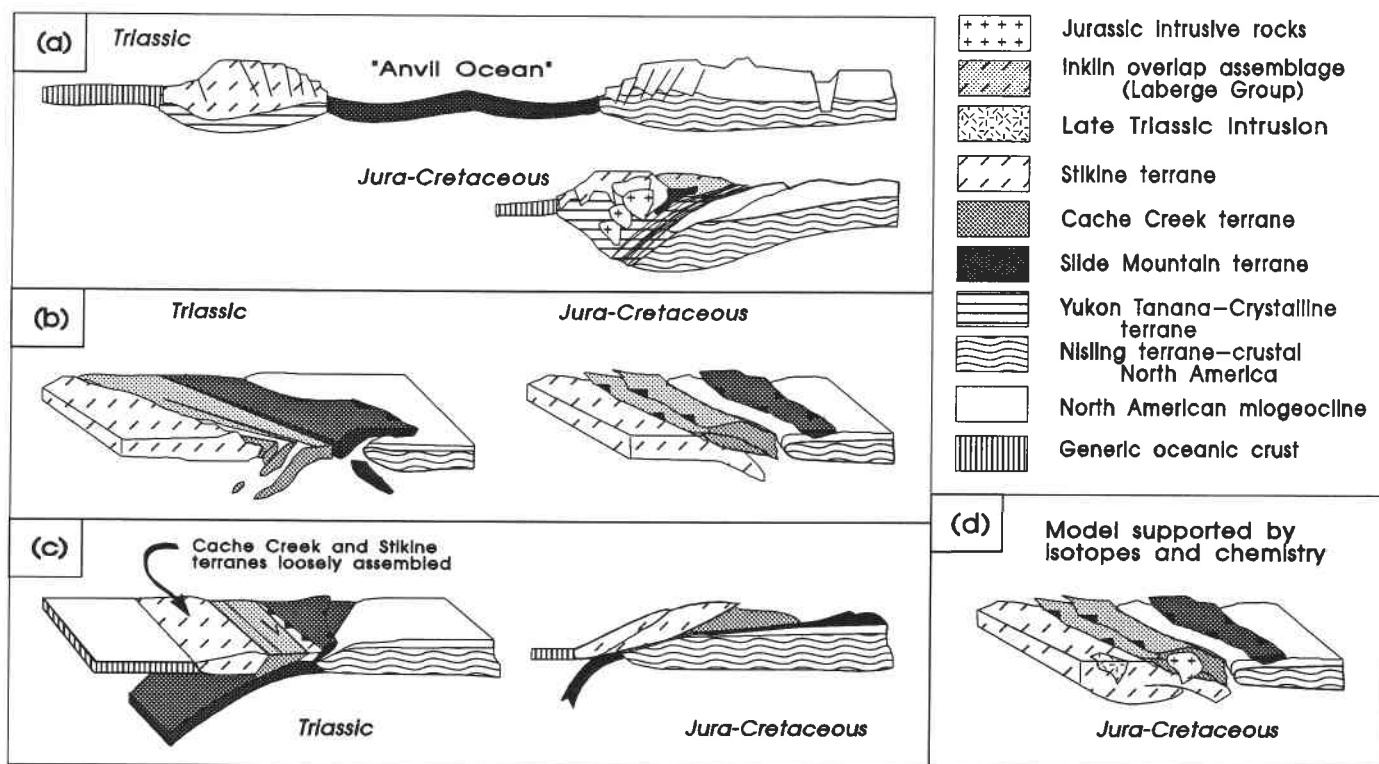
FIG. 2. Models that have been proposed to explain emplacement of the Cache Creek terrane in the northern Canadian Cordillera. (a) The continental rift and collapsed ocean basin model (Tempelman-Kluit 1979). (b) Amalgamation of outboard terranes through mainly northeastward transport of crustal fragments (Monger 1977). (c) Megathrusting of Stikine and Cache Creek terranes (Coney 1989; Hansen 1990; Gehrels et al. 1991b) over metamorphosed North American continental-margin assemblage. (d) Model most consistent with evidence from this study (modified from Monger 1977).

Wynne 1990) necessitated little latitudinal displacement. Minimum displacement is also more consistent with the apparent continuity of continental-margin strata that envelop the northern termination of the Cache Creek and Stikine terranes. To explain these observations several authors have proposed that the Stikine and Cache Creek terranes represent a large thrust sheet (now a klippe) emplaced eastward over deformed ancestral continental margin (now Nisling and Yukon–Tanana terranes; Coney 1989; Gehrels et al. 1991a, 1991b; Hansen 1990) (Fig. 2c).

Closure of the Cache Creek ocean basin and mainly southwestward obduction of the Cache Creek complex (hereafter referred to as emplacement) has only been indirectly dated. Overlap of Stikine and Cache Creek terranes by the Lewes River assemblage (Wheeler et al. 1988) suggests a distal stratigraphic link by Late Triassic time. However, in the Atlin–Bennett area, Cordey et al. (1991) identified Early Jurassic radiolarians of Pliensbachian or early Toarcian age in the Cache Creek terrane, coeval with the Laberge Group which elsewhere may unconformably overlay the Cache Creek terrane (Monger et al. 1991). Emplacement-related deformation near Dease Lake is dated as late Early to Middle Jurassic based on stratigraphic arguments (Toarcian to middle Bajocian; Thorstad and Gabrielse 1986). In the same area, a small pluton that yields K–Ar dates of approximately 160 Ma (hornblende) and 173 Ma (biotite) cuts southerly directed, emplacement-related thrust faults (Stevens et al. 1982).

We address the timing and mode of Cache Creek terrane emplacement and the character of the assemblages that presently underlie the Cache Creek terrane, using the U/Pb and Rb/Sr isotopic and trace element geochemical signatures of plutonic rocks that intrude the Cache Creek and Stikine terranes in the Atlin–Bennett area. Presuming that the magmatic rocks act as geochemical recorders of their deep crustal origins, it should be possible to distinguish between old radiogenic continental sources and relatively juvenile arc sources. Plutons investigated in this study were selected from a wide age range within known tectonic settings. They belong to three suites: Late Triassic granitoids that intrude the Stikine terrane; Mid-Jurassic plutons emplaced within the Cache Creek terrane; and Late Cretaceous to Eocene plutons that cut the western margin of the Cache Creek terrane. In addition, we analyzed rhyolites from the Table Mountain complex which overlies the Cache Creek terrane.

Geologic framework of the Atlin–Bennett area

Several tectonic elements are represented in the Atlin–Bennett area. From west to east, these include parts of the Nisling, Stikine, and Cache Creek terranes, as well as younger (post-Upper Triassic) strata that overlap the older terranes (Fig. 1b). Cache Creek terrane rocks in the study area consist of an oceanic lithospheric package of highly sheared, weakly metamorphosed basalt, breccia, chert, argillite, wacke, limestone, and ultramafic rocks of Mississippian to Late Triassic (Norian) age (Monger 1975; Bloodgood and Bellefontaine 1990; unpublished British Columbia Geological Survey data). Fossils of possible Toarcian age (ca. 187–178 Ma) have been recovered by Cordey et al. (1991) from a nearby area to the northeast. Arc-derived sediments of the Lower Jurassic

2466 CAN. J. EARTH SCI. VOL. 29, 1992

Laberge Group (Inklin overlap assemblage) are juxtaposed with the Cache Creek terrane across the Nahlin Fault but elsewhere may directly overlie the Cache Creek terrane (Wheeler *et al.* 1988). The Laberge Group is unconformably overlain by Paleocene felsic to intermediate volcanic and volcaniclastic rocks of the Sloko Group.

Volcanic strata unconformably overlie the Cache Creek terrane west of Atlin. These are divided, on the basis of field and isotopic evidence presented below, into an upper unit of felsic to intermediate flows, ashflows, and tuff (Table Mountain volcanic complex; Mihalynuk and Smith 1992) of Late Cretaceous age (72.4 ± 2 Ma Rb–Sr whole rock; Grond *et al.* 1984; and ages reported herein) and a lower, intermediate to mafic, epidote-altered unit of flows, tuff, and epiclastic rocks of possible Triassic or Jurassic age called the Peninsula Mountain suite (Mihalynuk and Smith 1992).

The Cache Creek and Stikine terranes are intruded by numerous felsic plutonic bodies. The oldest rocks analyzed here are from the Triassic Stikine plutonic suite (Anderson 1989), which intrude the Stuhini Group east of the Llewellyn fault (Fig. 1b). Stikine plutonic rocks comprise strongly foliated to nonfoliated, fault-dissected granodiorite and granite. They typically contain a greater abundance of hornblende than biotite and are K-feldspar porphyritic. Their distribution, lithologic variations, and contact relationships are described in more detail by Hart and Radloff (1990) and Mihalynuk and Mountjoy (1990).

Jurassic rocks include the Fourth of July batholith (Fig. 1b), a heterogeneous intrusive complex that varies from diorite to granite and alaskite. It is dominantly granite, with biotite- to hornblende-rich and K-feldspar megacrystic to equigranular phases. The exact age of the pluton is important because the batholith cuts and thermally metamorphoses deformed rocks of the Cache Creek terrane and has itself been subjected to only relatively minor, brittle deformation, and thus constrains the minimum age of deformation. It was originally regarded as Jurassic (Aitken 1959), until Christopher and Pinsent (1982) reported K–Ar cooling dates of 110 ± 4 Ma (hornblende) and 73.3 ± 2.6 Ma (biotite) from samples obtained from a part of the batholith immediately adjacent to the Surprise Lake batholith. Subsequent reports (e.g., Tipper *et al.* 1981; Wheeler and McFeely 1987; Bloodgood and Bellefontaine 1990) assigned a Cretaceous to early Tertiary age based on these dates. Analysis of common Pb in galena from the Surprise Lake batholith (Godwin *et al.* 1988) and K–Ar ages from a satellite pluton (Dawson 1988) and liswanitic and sericite altered rocks adjacent to the pluton (Ash *et al.* 1992) suggest a minimum age of between 160 and 170 Ma. Donelick (1988) obtained zircon fission-track dates of 128, 193, and 215 Ma.

The Mount McMaster stock (Fig. 1b), consisting of medium- to coarse-grained quartz diorite and granodiorite, has been correlated with the Fourth of July batholith based on lithologic similarities (Bloodgood and Bellefontaine 1990). Geochemical evidence supports this correlation (see below).

The Surprise Lake batholith intrudes both the Cache Creek terrane and the Fourth of July batholith. It consists of polyphase, texturally diverse alaskite, granite, and minor quartz monzonite. Constituents include smoky quartz, chalky albite, K-feldspar, and biotite (Bloodgood *et al.* 1989). The Surprise Lake batholith contains a variety of accessory minerals reflecting enrichment in U, W, Sn, and F, suggesting that it is chemically evolved (Ballantyne and Littlejohn 1982). An average K–Ar biotite age of 70.6 ± 3.8 Ma for six samples was reported by Christopher and Pinsent (1982).

The Birch Mountain pluton (Fig. 1b), consisting of leucocratic quartz monzonite with lesser diorite and gabbro, intrudes the Cache Creek terrane, Nahlin Fault, and Laberge Group (Bloodgood and Bellefontaine 1990). Bultman (1979) obtained K–Ar dates of approximately 46 Ma (hornblende) and 56 Ma (biotite) from this intrusion.

The Atlin Mountain pluton (Fig. 1b) intrudes the Cache Creek terrane, the Laberge Group, and the Peninsula Mountain volcanic suite; it both intrudes and is cut by a strand of the Nahlin Fault (Bloodgood and Bellefontaine 1990; Mihalynuk *et al.* 1992). This pluton is thus of considerable importance to investigation of the Cache Creek terrane and also to understanding subsequent strike-slip tectonics within the region. It consists of fine- to medium-grained, white-weathering quartz monzonite and was interpreted to be Tertiary in age by Aitken (1959).

Uranium–lead geochronology

Zircon fractions from four units were separated and analyzed: the Fourth of July batholith (two separate samples representing distinct phases), the Surprise Lake batholith, and an ash-flow tuff from the Table Mountain volcanic suite. Analytical results are listed in Table 1 and illustrated on concordia plots in Fig. 3. Appendix Table A1 provides zircon descriptions with locations.

Fourth of July batholith
MHG87-064
Four fractions were analyzed from this rock. The concordia plot (Fig. 3a) shows that all fractions are nearly concordant, but are 6 Ma apart, suggesting either minor lead loss or minor inheritance of older lead. Our interpretation of the age is based on lead loss from zircons in the two younger fractions, because the resulting date is consistent with previously determined common lead, potassium-argon, and argon-argon dates. An isochron constrained by a zero lower intercept yields an upper intercept date of 170.4 ± 5.1 (2σ) Ma, which represents the best estimate of the intrusive age of this phase (an unconstrained regression yields an impossible lower intercept). The maximum date for this sample is given by the ^{207}Pb/^{206}Pb date of the medium magnetic fraction, 174.1 ± 7.6 (2σ) Ma.

DVL87-082
Four zircon fractions were analyzed from a quartz syenite sample from the south end of the batholith (Fig. 3b). As with MHG87-064, all fractions overlap concordia. The best estimate of the age of this sample is 171.5 ± 3.4 (2σ) Ma, the upper intercept of an isochron constrained by an assumed zero lower intercept. An unconstrained regression yields intercepts of 176^{+31}_{-6} Ma and 72^{+72}_{-95} Ma. The upper intercept provides a maximum age constraint; however, we prefer the constrained date because the errors are more reasonable. If the discordia pattern is due to lead loss, the minimum age of intrusion is given by the weighted mean of the ^{206}Pb/^{238}U dates from the two nearly concordant fractions, at 166.6 ± 0.5 (2σ) Ma. These estimates are in accordance with the dates from MHG87-064.

Taken together, these data suggest that two phases of the Fourth of July batholith were intruded between 174 ± 7 and

TABLE 1. U–Pb analyses of zircon fractions from rocks in the Atlin area

Fraction	Weight (mg)	U (ppm)[a]	Pb (ppm)[a]	^{207}Pb	^{208}Pb ($^{206}Pb = 100$)	^{204}Pb	Measured $^{206}Pb/^{204}Pb$[b]	Blank Pb (pg)[c]	$^{206}Pb/^{238}U$	$^{207}Pb/^{235}U$	$^{207}Pb/^{206}Pb$	$^{206}Pb/^{238}U$	$^{207}Pb/^{235}U$	$^{207}Pb/^{206}Pb$
									Atomic ratio (± 1σ)			Age (Ma ± 1σ)		
FOURTH OF JULY BATHOLITH Quartz diorite, MHG87-064														
(a) NM, 1.9 A, 1°, +100	4.6	293	7.75	5.4186	13.884	0.0325	2845	50	0.02561±0.00025	0.1744±0.0017	0.04940±0.00008	163.0±1.5	163.3±1.5	167.1±3.7
(b) M, 1.9 A, 1°, −200	0.4	296	8.22	5.4488	13.707	0.0336	2044	30	0.02698±0.00007	0.1844±0.0005	0.04955±0.00008	171.6±0.4	171.8±0.4	174.1±3.8
(c) M, 1.9 A, 1°, −200	1.1	296	8.1	5.1404	13.021	0.0138	1668	25	0.02688±0.00007	0.1830±0.0008	0.04937±0.00015	171.0±0.4	170.6±0.7	165.7±7.2
(d) M, 1.5 A, 3°, −200 +325	0.4	267	7.38	6.2996	51.852	0.0929	820	50	0.02587±0.00009	0.1759±0.0008	0.04933±0.00017	164.6±0.6	164.6±0.7	163.5±7.9
Quartz syenite, DVL 87-082														
(a) NM, 2 A, 1°, +125	1.7	836	20.3	5.1868	11.586	0.0195	4539	50	0.02404±0.00037	0.1624±0.0022	0.04899±0.00041	153.1±2.3	152.8±1.9	148±20
(b) NM, 2 A, 1°, +125	1.2	835	17.5	5.0419	11.661	0.0048	9272	30	0.02085±0.00083	0.1414±0.0056	0.04919±0.00008	133.1±5.2	134.3±5.0	156.7±4.0
(c) M, 2 A, 1°, −125 +200	0.4	735	19.9	5.2387	11.875	0.0196	3864	30	0.02615±0.00005	0.1785±0.0004	0.04951±0.00004	166.4±0.3	166.8±0.3	172.1±1.7
(d) M, 1.5 A, 3°, −200	1.7	1079	29.1	5.2430	13.727	0.0202	4545	50	0.02624±0.00007	0.1790±0.0006	0.04946±0.00007	167.0±0.4	167.2±0.5	169.8±3.2
SURPRISE LAKE BATHOLITH Biotite granite, DVL87-051														
(a) NM, 2 A, 1°, +200	0.2	892	11.6	6.0738	11.043	0.0877	812	50	0.01267±0.00004	0.0835±0.0004	0.04781±0.00017	81.2±0.2	81.4±0.4	89.9±8.7
(b) M, 2 A, 1°, +200	0.5	4320	52.55	5.9152	9.005	0.0794	1222	30	0.01212±0.00006	0.0793±0.0005	0.04745±0.00011	77.7±0.4	77.5±0.4	72.1±5.5
(c) M 2 A, 1°, −200	0.2	1729	18.11	4.8180	7.001	0.0030	6268	30	0.01089±0.00002	0.0716±0.0002	0.04774±0.00004	69.8±0.1	70.3±0.2	86.4±2.1
(d) M, 1.5 A, 3°, −325	0.7	5277	61.8	5.3361	8.512	0.0385	2460	50	0.01187±0.00014	0.0781±0.0010	0.04769±0.00010	76.1±0.9	76.3±0.9	84.0±5.0
TABLE MOUNTAIN VOLCANIC SUITE Rhyolitic ash-flow tuff NW189-17-05														
(a) M 2 A, 1°, −125 +200	0.6	796	10.63	5.9410	14.453	0.0793	1146	30	0.01269±0.00006	0.0835±0.0004	0.04773±0.00009	81.3±0.4	81.4±0.4	85.7±4.5
(b) M, 1.5 A, 3°, −200	0.65	659	8.81	5.6195	15.423	0.0569	1513	30	0.01269±0.00004	0.0837±0.0003	0.04782±0.00005	81.3±0.2	81.6±0.2	90.2±2.3

NOTES: Analyses by J. E. Gabites (1990–1992) at the University of British Columbia. IUGS conventional decay constants (Steiger and Jäger 1977) are $^{238}U\lambda = 1.55125 \times 10^{-10}$ a^{-1}; $^{235}U\lambda = 9.8485 \times 10^{-10}$ a^{-1}; $^{238}U/^{235}U = 137.88$ atomic ratio. Side slope is given in degrees. −, crystals are smaller than the stated mesh; +, crystals are larger than the stated mesh. M and NM, magnetic and nonmagnetic at given amperes on magnetic separator. Zircon fractions are abraded and labelled according to magnetic susceptibility and size. General procedure: Zircons are separated using standard mechanical, wet shaking table, heavy liquid, and magnetic techniques, sized using new nylon mesh screens, hand picked, and air abraded (Krogh 1982). Chemical dissolution and mass spectrometry follow the procedures of Krogh (1973). A mixed ^{205}Pb–^{233}U–^{235}U spike is used (Parrish and Krogh 1987; Roddick et al. 1987). The dissolution is in small-volume teflon capsules contained in a large Parr bomb (Parrish 1987). A Daly collector is used to improve ^{204}Pb signals. U–Pb date errors are obtained by individually propagating all calibration and measurement uncertainties through the entire date calculation and summing the individual contributions to the total variance (Nunes 1980). Concordia intercepts are based on York (1969) regression and Ludwig (1980) error algorithm. Errors shown on concordia plots are 2σ (95% confidence limits).

[a]U and Pb concentrations are corrected for blank U and Pb. Laboratory blanks for U and Pb are approximately 6 ± 0.5 and 30 ± 10 pg based on ongoing analyses of total procedural blanks. A larger value may have been used in data reduction in some cases (see column entitled Blank Pb).

[b]Common Pb is assumed to be Stacey and Kramers (1975) model Pb of 170 ± 10 Ma age for Jurassic samples and 90 ± 10 Ma age for Cretaceous samples.

[c]Isotopic composition of laboratory blank is 206:207:208:204 = 17.75:15.50:37.30:1.00, based on ongoing analyses of total procedural blanks.
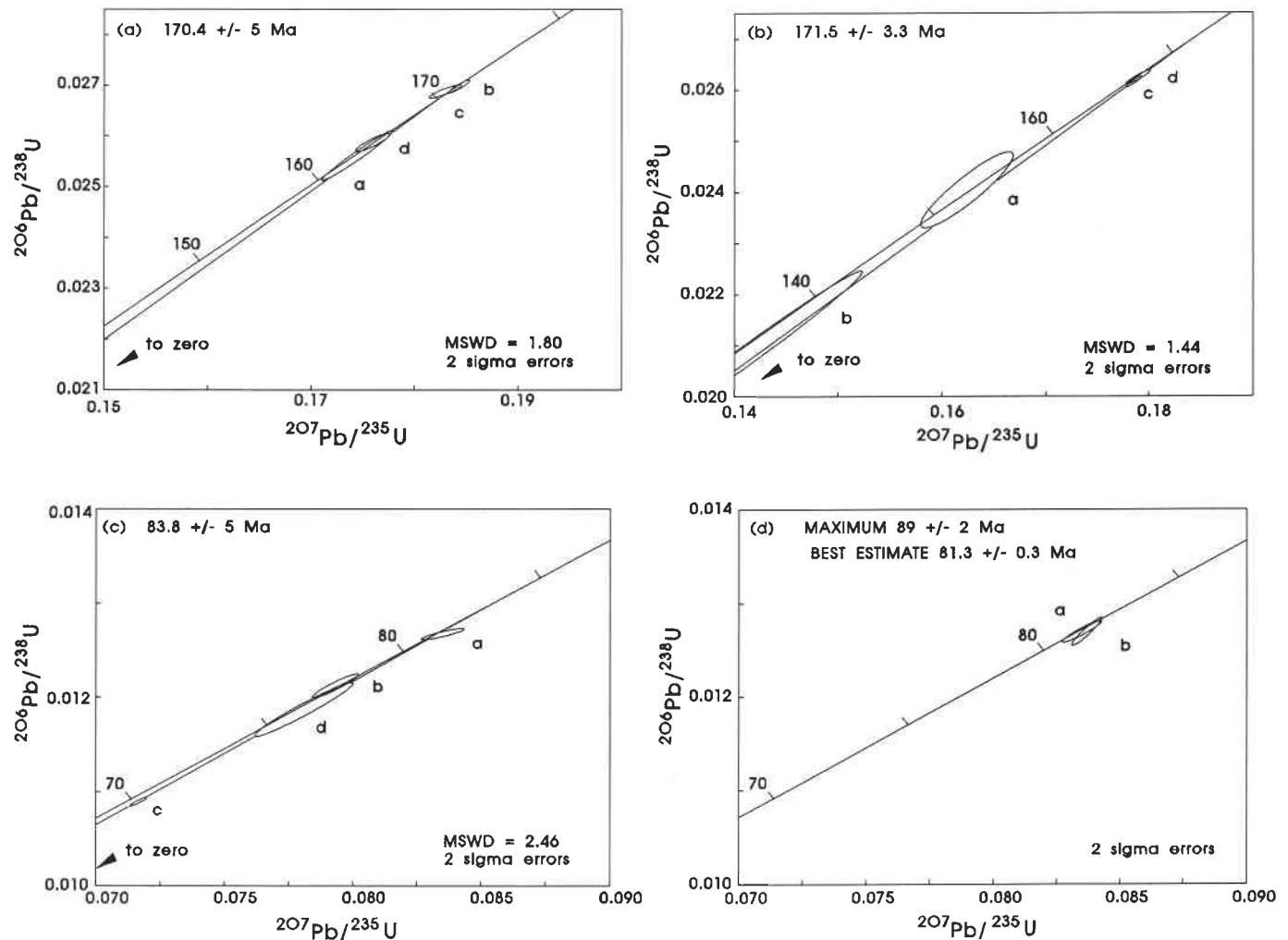
FIG. 3. $^{206}Pb/^{238}U$ vs. $^{207}Pb/^{235}U$ concordia plots for (a) sample MHG87-064, Fourth of July batholith; (b) sample DVL87-082, Fourth of July batholith; (c) sample DVL87-051, Surprise Lake batholith; and (d) sample NWI89-17-5, a rhyolite from the Table Mountain volcanic suite. Lower-case letters refer to fractions identified in Table 1.

166.6 ± 0.5 Ma, with best age estimates of 170.4 and 171.5 Ma (indistinguishable within error estimates). If the two phases are indeed coeval, the combined data yield an isochron best estimate of 171.7 ± 3 Ma.

Surprise Lake batholith

A concordia plot for DVL87-051 (Fig. 3c) shows that three of four fractions overlap concordia and are spread between 81 and 69 Ma. We interpret this pattern to be due to lead loss from the finer fractions, which are significantly richer in uranium than the coarse nonmagnetic fraction. A minimum age assuming lead loss is given by the $^{206}Pb/^{238}U$ date from the oldest fraction, at 81.2 ± 0.2 (2σ) Ma. The best estimate of the age of this rock is the upper intercept of an isochron constrained by an assumed zero lower intercept (an unconstrained regression yields an impossible negative lower intercept). This date is 83.8 ± 5 (2σ) Ma, equivalent to the weighted mean of the $^{207}Pb/^{206}Pb$ dates from the four fractions.

Table Mountain volcanic suite

Two fractions analyzed from a rhyolite ash flow collected from north of Graham Inlet overlap concordia (Fig. 3d). The best estimate of the age of the rock is 81.3 ± 0.3 (2σ) Ma, the mean of the two $^{206}Pb/^{238}U$ dates. A maximum age is given

by the weighted mean of the $^{207}Pb/^{206}Pb$ dates, at 89 ± 2 (2σ) Ma. This sample yields the same date (within analytical errors) as that of the Surprise Lake batholith.

Rb–Sr analyses

Rb–Sr isotopic ratios and elemental abundances were determined on samples of five plutonic bodies that intrude the Cache Creek terrane and two ash-flow units from the Table Mountain volcanic suite. Apparent age estimates and initial ratios were calculated from two- and three-point whole-rock isochrons for each sample set (Table 2).

It is not possible to calculate reliable Rb–Sr dates from two points for either the Fourth of July batholith or Mount McMaster pluton because of insufficient spread in the $^{87}Rb/^{86}Sr$ ratios (Fig. 4a; Table 2). For example, two samples from the Fourth of July batholith give an isochron date of 249 ± 26 Ma, which is older than the rocks it intrudes. If the age of intrusion is taken as the U–Pb age of approximately 172 Ma, a corrected initial $^{87}Sr/^{86}Sr$ ratio can be calculated (Steiger and Jäger 1977). Initial ratios calculated in this manner are reported in Table 2 and for the Fourth of July batholith are 0.7038 and 0.7039. Previous geochronometry from the Mount McMaster pluton produced a K–Ar biotite date of

TABLE 2. Rb−Sr data for samples from the Atlin area

Number in Fig. 4	Sample no.	Rock type	Sr^a (ppm)	Rb (ppm)	$^{87}Rb/^{86}Sr^b$	$^{87}Sr/^{86}Sr^c$ ($\pm2\sigma \times 10^{-5}$)	Date (Ma $\pm 2\sigma$)	$^{87}Sr/^{86}Sr_i$ from two-point isochron	U−Pb age (Ma)	$^{87}Sr/^{86}Sr_i$ calculated from U−Pb age
		FOURTH OF JULY BATHOLITH								
1-a	DVL-87-82	Quartz syenite	988	113	0.330	0.70459±4	249±13	0.70342±8	172	0.7038
1-b	KAB137	Granite	739	130	0.509	0.70523±4			172	0.7039
		MOUNT MCMASTER PLUTON								
2-a	MAB89-238	Granodiorite	709	54	0.220	0.70468±3			172	0.7041
2-b	MAB89-233	Granodiorite	824	63	0.219	0.70466±3			172	0.7041
		ATLIN MOUNTAIN PLUTON								
3-a	ICG41	Quartz monzonite	365	129	1.018	0.70567±5	75±28	0.70458±37		
3-b	ICG42	Quartz monzonite	393	117	0.862	0.70550±3				
		TABLE MOUNTAIN VOLCANIC ROCKS								
4-a	MMI89-17-3	Biotite feldspar ash flow	283	116	1.183	0.70566±4	75.3±2.7	0.70441±4	81.3	0.7042
4-b	KMO90-13-7a	Quartz eye ash flow	532	57	0.307	0.70474±6			81.3	0.7043
4-c	T75 305-8^d	Rhyolite	64.7	180	8.05	0.7131±20				0.7037
		BIRCH MOUNTAIN PLUTON								
5-a	LOU54	Granite	155	156	2.908	0.70667±4	50.4±4.5	0.70459±24	58	0.7042
5-b	LOU68	Granite	67	134	5.782	0.70873±3				0.7039
		SURPRISE LAKE BATHOLITH								
6-a	CRE228	Alaskite	34.1^e	465^e	39.6	0.74712±4	72.2±0.8	0.70647±62	83.8	0.6999
6-b	ICG54	Alaskite	5.24^e	539^e	306.9	1.02152±8			83.8	0.6552

NOTES: All samples were analyzed as whole rocks by Dita Runkle at the University of British Columbia. Rb and Sr concentrations are determined by replicate analyses of pressed powder pellets using X-ray fluorescence. (XRF) Mass absorption coefficients are obtained from Mo K-alpha Compton scattering measurements. Sr isotopic composition is measured on unspiked samples prepared using standard ion exchange techniques. The Sr isotopic measurements are made on a VG 54R mass spectrometer automated with an HP-85 computer. The precision of a single $^{87}Sr/^{86}Sr$ ratio is 0.0001 (1σ) unless noted. Blanks for Rb and Sr are approximately 0.8 and 6 ng, respectively. Regressions are calculated according to the technique of York (1967).

^{a}Sr and Rb concentrations by XRF have ±1 standard deviation errors of 5%.

^{b}$^{87}Rb/^{86}Sr$ ratios by XRF have ±1 standard deviation error values of 2% for samples with both concentrations over 50 ppm and $^{87}Rb/^{86}Sr$ divided by the lowest concentration for samples with concentrations below 50 ppm (effectively ±1 ppm lower limit on concentration uncertainty).

^{c}The ±1 standard deviation errors for $^{87}Sr/^{86}Sr$ are for mass spectrometer measurements. Measured ratios have been normalized to a $^{86}Sr/^{88}Sr$ ratio of 0.1194 and adjusted so that the National Bureau of Standards standard $SrCO_3$ (SRM 987) gives a $^{87}Sr/^{86}Sr$ ratio of 0.71019 ± 0.00002 and the Eimer and Amend Sr standard a ratio of 0.70800 ± 0.00002. $\lambda = 1.42 \times 10^{-11}$ a^{-1} (Steiger and Jäger 1977).

^{d}Analysis reported in Grond et al. (1984).

^{e}Determination by isotope dilution, using ^{84}Sr and ^{87}Rb spikes to obtain concentrations with a precision of 1.5%. The precision of the Rb/Sr ratio is ~2%.

60 ± 18 Ma (Wanless et al. 1972); however, lithologic characteristics, rare-earth element (REE) patterns, and Rb and Sr elemental abundances are much like those of the Fourth of July batholith, and we consider them to be comagmatic. Thus we have an assumed age of 172 Ma in order to calculate an initial ratio 0.7041. A younger age would produce a slightly higher initial ratio.

Rb−Sr dates calculated from two- and three-point isochrons for the Birch Mountain and Atlin Mountain plutons and Table Mountain volcanic suite are more geologically reasonable ages (Fig. 4b). The date from the Atlin Mountain pluton is 75 ± 28 Ma (falling within constraints imposed by field relations) with a corresponding initial ratio of 0.7046. No previous dates have been reported from this intrusion. The Birch Mountain pluton date (50.4 ± 4.5 Ma) is approximately in agreement with previous hornblende and biotite K−Ar dates of 48 ± 1.1 and 58 ± 1.1 Ma, respectively, obtained from a single sample (Bultman 1979). The corresponding initial ratio is 0.7046. If the biotite date (58 Ma) is assumed to be a more reliable representation of the age of the pluton, the calculated initial ratios are 0.7042 and 0.7038. The two samples from the Table Mountain volcanic suite produced a date of 73.4 ± 6 Ma. A

recalculation was made including the Table Mountain sample (T75 305-8) published by Grond et al. (1984). The result of the three-point isochron is a date of 75.3 ± 2.7 Ma, approximately 6 Ma younger than the U−Pb age. The calculated initial ratios based on this U−Pb age range from 0.7039 to 0.7042, perhaps reflecting heterogeneity within the Table Mountain volcanic suite.

$^{87}Sr/^{86}Sr$ and $^{87}Rb/^{86}Sr$ ratios for the Surprise Lake batholith are considerably higher than any others reported here, reflecting the chemically evolved nature of this intrusion (Ballantyne and Littlejohn 1982). The two-point isochron date is 72.2 ± 0.8 Ma, similar to K−Ar biotite dates (Christopher and Pinsent 1982) and corresponding to an initial $^{87}Sr/^{86}Sr$ ratio of 0.7065 ± 0.0006 (Fig. 4c). However, if the age of the batholith is taken to be 84 Ma (the U−Pb age), it yields geologically unreasonable initial ratios of 0.6999 and 0.6552, indicating open-system behavior.

In summary, the Rb−Sr two-point isochrons do not yield particularly reliable age information, as the dates are either consistently several million years younger than the U−Pb ages or (in the case of the Jurassic intrusions) are in error because the points are too close together. Dates on the younger
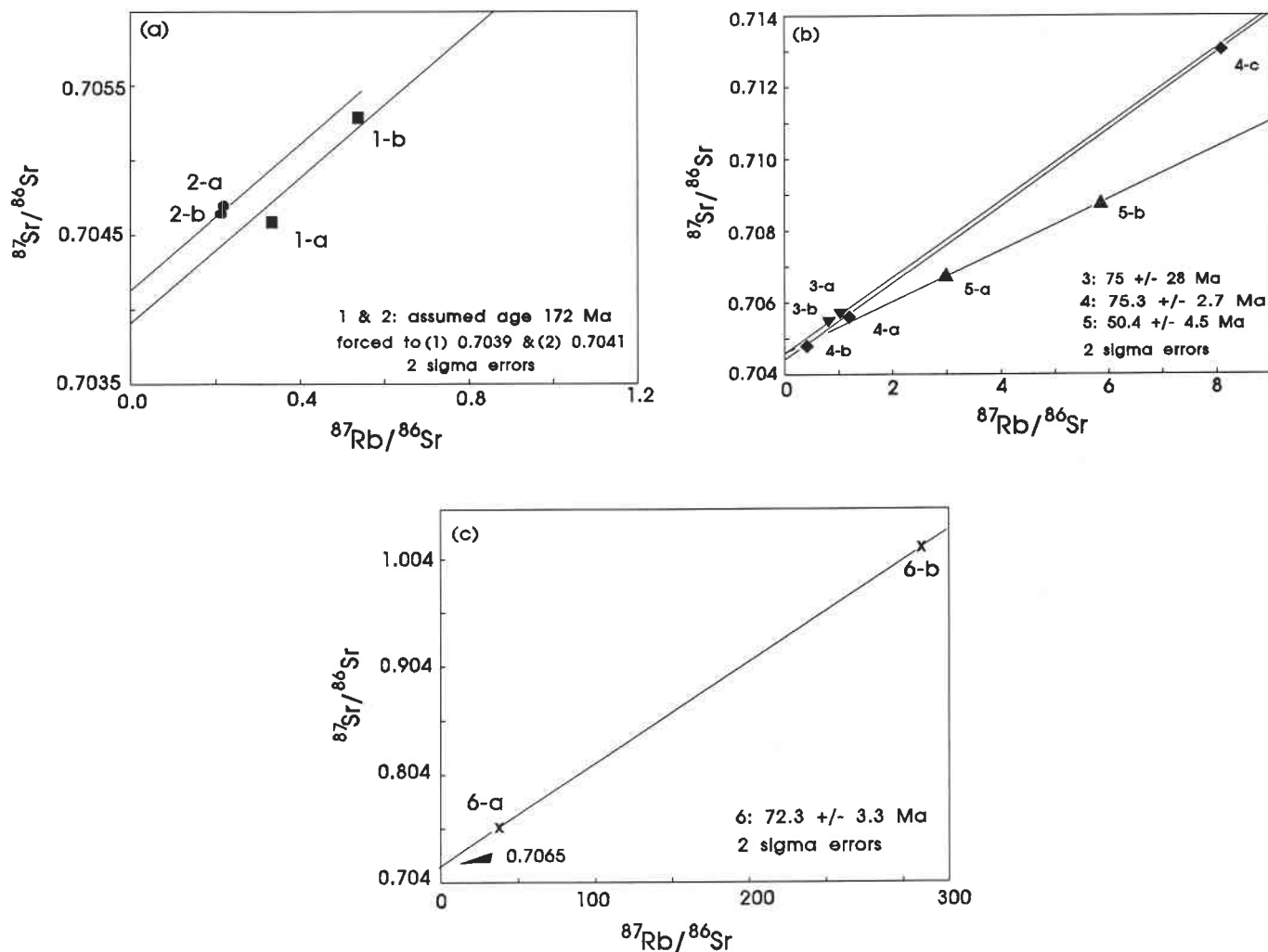
FIG. 4. Rb/Sr isochron plots for samples from (a) the Jurassic Fourth of July batholith and Mount McMaster pluton; (b) the Cretaceous and younger Atlin Mountain pluton, Table Mountain Volcanic suite, and Birch Mountain pluton; and (c) the Surprise Lake batholith. Data are listed in Table 2. Letters and numbers correspond to those in Table 2.
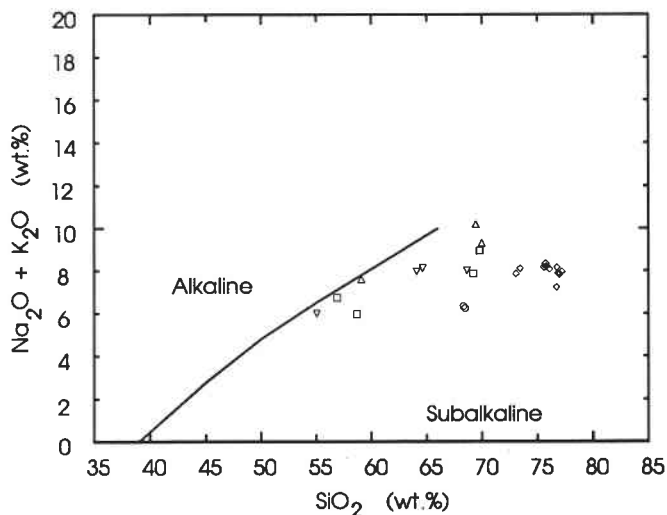
FIG. 5. Alkali-silica plot (Irvine and Barager 1971) of intrusions of the Atlin–Bennett area. Rocks of high SiO_2 content belong to the calc-alkaline series.

plutons that are lower than U−Pb ages may reflect minor alteration of the rocks. With the exception of the unreliable Surprise Lake data, initial ratios, whether calculated from two-point isochrons or from U−Pb ages, are consistently between 0.7038 and 0.7046, suggesting derivation from a relatively unevolved source.

Trace element geochemistry

$^{87}Sr/_{86}Sr$ initial ratios have been repeatedly shown to outline the degree of involvement of continental lithosphere in granitoid source region (e.g., Kistler and Peterman 1978) but generally do not permit discrimination between other types of source areas. Effective source area discrimination typically relies on schemes that utilize immobile trace and rare-earth elements (e.g., Pearce *et al.* 1984; Whalen *et al.* 1987) including the high-field-strength (HFS) elements Ta, Nb, Hf, Zr, and Y. Large-ion lithophile elements (LILE) (Saunders and Tarney 1984) such as K, Rb, U, Th, Cs, Sr, and Ba are, with the exception of Th, relatively mobile. However, field and petrographic evidence for significant alteration of the Atlin granitoids is lacking, so it is unlikely that interpretations
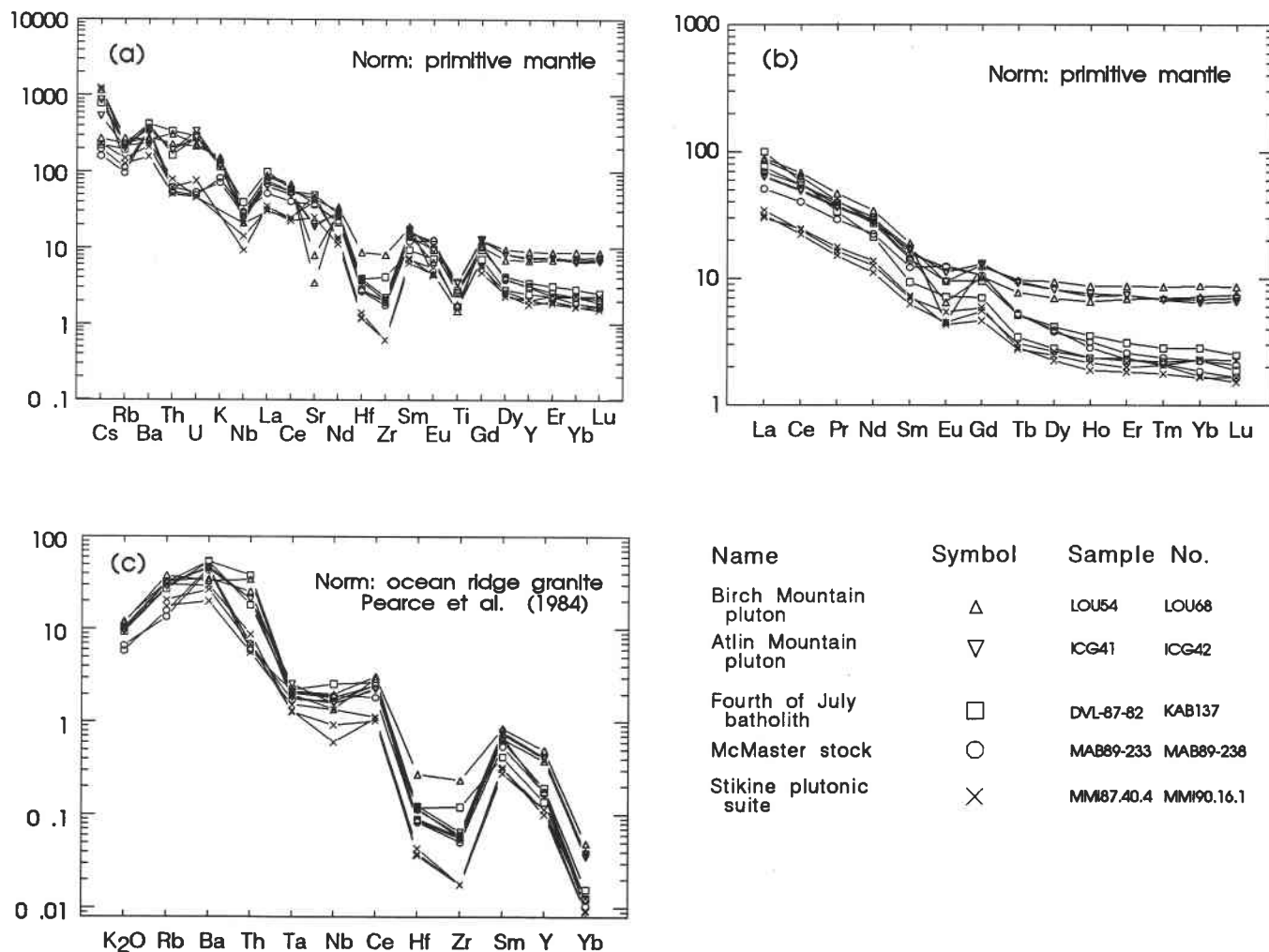
FIG. 6. (a) Extended REE plot for granitic bodies in the Atlin–Bennett area. Normalizing factors are those of primitive mantle (Taylor and McLennan 1985). (b) REE plot showing enrichment in light REE and depletion of heavy REE. Greater depletion of heavy REE in the Middle Jurassic suites serves to distinguish them from the Late Cretaceous to Paleocene intrusions. (c) Elements that behave incompatibly during the fractionation of mid-ocean-ridge basalts are shown normalized to hypothetical ocean-ridge granite by the method of Pearce et al. (1984).

involving LILE's are flawed in this regard. A geochemical indication of the lack of alteration is shown by the consistency of Rb or Sr concentrations from sample to sample within a particular pluton. For example, $^{87}Rb/^{86}Sr$ and $^{87}Sr/^{86}Sr$ ratios obtained from separate samples of the Fourth of July batholith are very similar, and from samples of the Mount McMaster body they are nearly identical (Table 2).

Trace and rare-earth element concentrations were determined for 11 samples from seven granitoids bodies belonging to the three calc-alkaline (Fig. 5) suites (Early Triassic, Mid-Jurassic, and Late Cretaceous – early Tertiary) described above (Fig. 1). These are compared in the three spidergrams of Fig. 6.

REE's are generally incompatible with mineral phases that fractionate during derivation of a granitic magma from a more mafic melt. As a result, granitoids tend to be enriched in these elements. An extended element plot (Fig. 6a) illustrates this well, as all elements but Zr display abundances greater than those of primitive mantle. Light REE are generally 3 – 100× enriched, whereas heavy REE are 1.6 – 10× primitive mantle abundances. All samples are also highly enriched in LILE's

(Figs. 6a, 6c) and display relative correlated Zr and Hf. A correlated depletion of Zr and Hf is likely a result of zircon fractionation (Harris et al. 1984; Pearce et al. 1984; incomplete zircon digestion during the dissolution procedure could also explain this trend, except that no residue was observed).

A striking feature of every plot is the volcanic-arc granite (VAG) character of all the geochemical patterns displayed (Fig. 6c). All display a suprasubduction zone component, which is particularly evident when normalized with respect to hypothetical ocean-ridge granite (ORG) and compared with the patterns of Pearce et al. (1984).

Subtle differences between the suites do exist. Most obvious is the depletion in heavy REE of the Middle Jurassic and older suites with respect to the younger intrusives. $(Gd/Lu)_N$ correlates roughly with age, from 1.37 in the youngest granitoids to 6.35 in the McMaster stock (Table 3). Stuhini arc granitoids have REE that are slightly lower overall than those that intrude the Cache Creek terrane. Both the Mount McMaster stock and the Stuhini arc granitoids are slightly depleted in Th and U with respect to the more northern Cache Creek suites. Finally, the Birch Mountain intrusion displays relative Sr depletion.

TABLE 3. Trace and rare-earth element

	Late Cretaceous to Eocene suite				Middle
No. in Fig. 1:	L54	L68	I42	I41	L82
Sample no.:	LOU54	LOU68	ICG41	ICG42	DVL87-082
Geologic unit:	Birch Mountain	Birch Mountain	Atlin Mountain	Atlin Mountain	Fourth of July
Rb	151	129	125	114	108
Cs	8.21	1.90	6.06	3.73	1.54
Ba	1638	1745	2231	2335	2635
Sr	150	65	359	387	949
Ti	1.12	0.58	0.88	0.78	0.53
Ta	1.37	1.49	1.79	1.30	1.43
Nb	13.6	19.8	15.6	15.9	18.1
Hf	1.04	2.43	1.11	1.01	0.80
Zr	19	79	22	20	19
Y	26	35	29	28	13
Th	27.32	20.20	16.82	16.61	14.40
U	4.95	4.68	6.17	7.46	6.04
La	53.93	55.77	40.59	39.99	48.07
Ce	101.27	108.70	79.93	78.29	86.96
Pr	10.30	11.79	9.27	9.10	9.56
Nd	34.32	41.45	35.25	34.02	33.00
Sm	5.90	7.59	6.98	6.64	5.66
Eu	0.97	0.68	1.42	1.68	1.43
Gd	5.48	6.65	6.85	6.99	5.09
Tb	0.76	0.95	0.92	0.90	0.50
Dy	4.60	6.24	5.41	5.43	2.77
Ho	0.97	1.29	1.13	1.07	0.52
Er	2.98	3.76	3.19	3.19	1.35
Tm	0.48	0.58	0.46	0.46	0.19
Yb	3.19	3.88	3.04	2.86	1.26
Lu	0.50	0.57	0.46	0.44	0.17
SiO_2	69.99	69.45	64.65	64.12	66.46
K_2O	4.61	4.84	3.93	3.76	3.70
Ba/Ta	1198	1173	1246	1799	1843
$(Gd/Lu)_N$	1.37	1.45	1.83	1.99	3.82

NOTES: All trace and REE analyses reported in ppm. Detection limits are generally about 0.01 ppm for REE and less abundant trace elements. Oxides in wt.%. Analytical procedure includes (*i*) digestion with HF/HNO_3 of a 0.1 g sample aliquot; (*ii*) analysis of the solution by inductively coupled plasma mass spectroscopy (ICP−MS), correcting for matrix effects using the method of standard addition; (*iii*) dissolution of insolubles with HCl/HNO_3. Phases resistant to digestion, particularly zircon, may not dissolve completely, in which case Zr and Hf values are minima. However, no solubles were encountered in these samples.

Tectonic discrimination

Despite minor chemical differences, the patterns are permissive of the same or a similar source area for all of the intrusive suites. Furthermore, the magmatic processes that accompanied the emplacement of each intrusive suite may have been similar (e.g., degree of assimilation, fractionation, volatile fluxing). Such similarity is notable, given (*i*) the spectrum of intrusive ages represented, (*ii*) the variability of the terranes into which the intrusions were emplaced, and (*iii*) the variety of major tectonic events that affected the region between the oldest and youngest intrusion dates.

Several features of the trace and REE patterns (Fig. 6) help discriminate the tectonic setting and affinity of the granitoids. In general, the patterns displayed by the samples are most like that of calc-alkaline volcanic-arc granites (Pearce *et al.* 1984): K, Rb, Ba, Th, Ce, and Sm show enrichment relative to Ta, Nb, Hf, Zr, Y, and Yb (Fig. 6c). Negative slopes from Hf to Yb on ORG-normalized plots as well as low values of Y and Yb are also considered characteristic of VAG's (Spell and Norrell 1990). On a Nb−Y plot (Fig. 7a), most samples fall within the VAG and syncollisional granite (syn-COLG) field. Separation of VAG from syn-COLG for these samples is

achieved on the Rb−(Y + Nb) diagram (Fig. 7b) in which samples plot in the VAG fields. Both diagrams effectively discriminate within-plate granites (WPG) from VAG and syn-COLG. Rb−(Yb + Ta) and Ta−Yb plots (not shown here) are similarly used to discriminate between VAG and syn-COLG. Samples plotted on the Ta−Yb diagram straddle the boundary between the two fields, but the Rb−(Yb + Ta) indicates a VAG source. Thus, both multielement spidergram plots and Nb−Y−Rb (and Rb−Yb−Ta) diagrams point to VAG source regions for the magmas. A VAG source is further indicated by Ba/Ta ratios greater than 450 (923−1868, Table 3), which according to Gill (1981) is a diagnostic geochemical characteristic of an arc magma.

Despite indications of VAG affinity for all samples, only the Stikine plutonic suite clearly intrudes comagmatic extrusive rocks of a volcanic-arc setting. All younger granites are postcollisional (as discussed above). Postcollisional granites do not necessarily correspond to the tectonic regime in which they are formed and can plot within syn-COLG, VAG, or WPG fields depending on the relative proportions and nature of mantle and crust involvement (Pearce *et al.* 1984) and enrichment−depletion factors later affecting the magma. Similarities between the

data for plutons in the Atlin – Bennett area

Jurrasic suite			Stikine plutonic suite		
K137 KAB137 Fourth of July	B233 MAB89-233 Mount McMaster	B238 MAB89-238 Mount McMaster	M16.1 MMI90.16.1 Stuhini arc	M40.4 MMI87.40.4 Stuhini arc	M2.5 MMI89.2.5 Stuhini arc
126	62	53	70	120	82
5.51	1.38	1.12	8.17	8.66	1.63
2683	2260	2153	988	1478	1321
716	817	696	778	470	912
0.94	0.39	0.44	0.53	1.08	0.31
1.56	1.21	1.49	1.07	0.89	0.91
25.7	16.8	18.9	13.5	9.2	6.0
1.07	0.77	0.75	0.33	0.34	0.39
41	19	17	6	6	6
10	12	12	7	8	8
30.00	5.47	4.70	4.45	7.01	5.44
6.33	1.17	1.07	1.00	1.02	1.68
63.04	43.62	32.22	18.93	19.82	21.76
92.72	87.01	63.97	39.09	35.68	38.48
8.50	10.05	7.32	4.42	3.81	4.13
25.86	36.82	27.21	16.62	13.42	15.34
3.76	6.23	4.89	2.91	2.50	2.80
1.08	1.84	1.87	0.65	0.68	0.82
3.78	5.64	5.66	2.48	2.96	3.15
0.34	0.51	0.51	0.27	0.3	0.28
1.86	2.60	2.52	1.63	1.76	1.49
0.35	0.42	0.47	0.32	0.35	0.28
0.98	1.00	1.12	0.86	1.02	0.79
0.15	0.14	0.16	0.14	0.14	0.12
1.00	0.82	1.00	0.75	1.02	0.73
0.13	0.11	0.14	0.10	0.15	0.11
69.83	68.33	68.50	—	—	—
4.12	2.31	2.63	—	—	—
1722	1868	1445	923	1661	1452
3.74	6.35	5.08	3.07	2.44	3.55

geochemical patterns of all samples suggest that they are a product of an established arc-intrusive repository, such as that produced in a zone of melting, assimilation, storage, and homogenization (MASH) as envisaged by Hildreth and Moorbath (1988). If MASH zones are indeed operative in arc environments, long-term episodic additions of magma to the Triassic Stuhini arc and its late Paleozoic arc substrate (Stikine assemblage; e.g., Currie 1992) could have established a crustal reservoir sufficient to dominate the REE budget. Such a reservoir would retain an arc signature only if non-arc basement is not also an important contributor. Consistency of REE patterns in all intrusive rocks studied points to involvement of primarily arc basement. Such consistent patterns do not support the presence of a significant evolved crustal source at depth.

Discussion

U – Pb data for the Fourth of July batholith suggest a crystallization age of 166.5 – 174 Ma, with a combined isochron best estimate of 171.7 ± 3 Ma. The batholith cuts and contact metamorphoses deformed rocks of the Cache Creek terrane and has itself only been subjected to relatively minor, brittle deformation. Thus the age of imbrication and obduction of the Cache Creek terrane over the Stikine terrane in the Atlin area is Middle Jurassic or earlier, consistent with fossil age data from within the Cache Creek terrane (Cordey et al. 1991) and the age of southwest-verging thrusts outboard of the northern Cache Creek terrane (Thorstad and Gabrielse 1986). The isotopic age, in conjunction with fossil ages, restricts the timing of this event in the Atlin area to late Toarcian through earliest Bajocian (ca. 183 – 171 Ma; Harland et al. 1990).

$^{87}Sr/^{86}Sr$ initial ratios for granitoids (exclusive of the Surprise Lake) in the Atlin – Bennett area range from 0.7039 to 0.7046. These fall within the range of values commonly observed in oceanic-island basalt and island-arc volcanic rocks (e.g., Faure 1986) and are consistent with derivation from the upper mantle, oceanic crust, or relatively young, continentally derived sources. A generally accepted lower boundary for Sr initial ratios in intrusive rocks intruded through rocks of continental affinity in western North America is approximately 0.706 (Kistler and Peterman 1978) and most granites that are continentally derived (S-type) have substantially higher (>0.708) values (White and Chappell 1983). Thus, the values obtained in this study would appear to be too low for deriva-
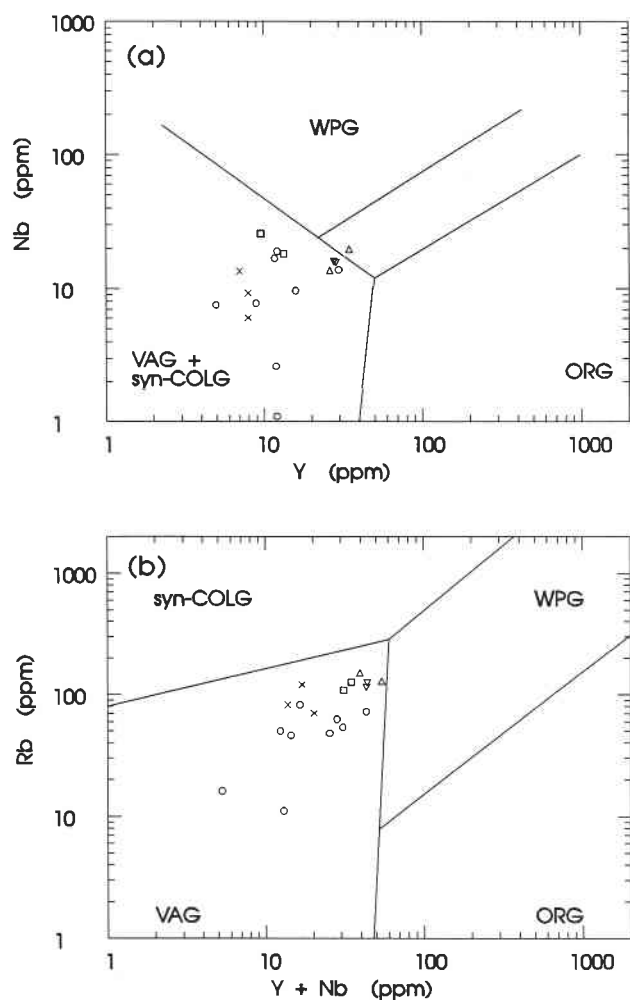
FIG. 7. (a) Nb−Y plot; most samples fall within the volcanic-arc granite (VAG) and syncollisional granite (syn-COLG) fields (Pearce et al. 1984). ORG, ocean-ridge granite; WPG, within-plate granite. (b) Rb−(Y + Nb) plot; serves to discriminate between syn-COLG and VAG.

tion of the magma from melting of old radiogenic crust, or even significant contamination by a significant proportion of such rocks during magma ascent. Similar Sr initial ratios were obtained by Morrison et al. (1979) on Mesozoic to Cenozoic plutons in the "Intermontane belt" (in part Cache Creek terrane) in the Whitehorse area to the north and by Armstrong (1988) to the south (Fig. 1b).

The Surprise Lake batholith $^{87}Sr/^{86}Sr$ initial ratio calculated from the two-point isochron is 0.7065, but back calculated from the U−Pb age of 83.8 Ma it averages 0.678, clearly indicating isotopic disturbance. This disturbance is apparently not random, as it affects the Table Mountain volcanic suite. Interpreted U−Pb zircon crystallization ages of the felsic Table Mountain volcanic suite and the Surprise Lake batholith are coeval within error (81.3 ± 0.2 and 83.8 ± 5.6 Ma, respectively) and may thus be comagmatic. Their Rb−Sr apparent ages are 75.3 ± 2.7 and 72.3 ± 0.8 Ma, respectively, and compare well with K−Ar biotite cooling ages from the Surprise Lake batholith that cluster between 75.4 ± 2.5 and 70.3 ± 2.4 Ma (five dates, Christopher and Pinsent 1982), recording coeval isotopic disturbance. One interpreta-

tion is that the Surprise Lake batholith took 10 Ma to cool and the Table Mountain suite was erupted near the end of the cooling episode. Fluid fluxing and volatile scavenging from late Paleozoic and early Mesozoic arc crust during such an unusually long cooling history might account for the generally evolved minor element chemistry of the batholith (e.g., elevated Rb, Sn, F, W, and Be; Ballantyne and Littlejohn 1982) rather than attributing this chemistry to inheritance from an evolved crustal source. Also inconsistent with derivation from subjacent old continental margin strata of the Nisling terrane is a lack of modal muscovite (White et al. 1976) as well as both older and younger adjacent plutons that are chemically and isotopically primitive.

U−Pb isotopic ratios are also consistent with this conclusion. The dates are essentially concordant and do not appear to reflect derivation from or significant contamination by early Paleozoic or older rocks. Plutonic rocks that intrude the Nisling terrane to the west of the study area do show this relationship. For example, an upper intercept of ~2070 Ma is calculated for the 61.5 ± 1.5 Ma Mendenhall pluton (Gehrels et al. 1991a), and Sloko Group volcanic rocks, locally containing Nisling schist clasts are dated at ca. 56 Ma but display a ca.1500 Ma inheritance (M. G. Mihalynuk, unpublished data).

REE and trace element chemistry suggest an established source region of arc character for all Atlin−Bennett area granitoids analyzed. One possibility is that episodic additions of magma during late Paleozoic to Triassic arc-building episodes produced a crustal reservoir (MASH; Hildreth and Moorbath 1988) of arc character present over a broad area beneath Stikinia. This crustal reservoir probably also extends beneath most of the Cache Creek terrane as a result of the emplacement of the Cache Creek terrane westward over the Stikine terrane prior to Middle Jurassic plutonism, probably late in the Early Jurassic.

From the standpoint of gross geometry, this model (Fig. 2d) is most similar to that of Monger (1977, shown schematically in Fig. 2c). Obduction arising from collapse of an oceanic basin between an arc and a continental margin can result in emplacement of the ophiolitic assemblage atop the associated arc complex, as is well documented for the Josephine Ophiolite in California (Harper 1984).

Conclusions

REE and trace element chemistry, isotopic data, and geologic relationships presented here are consistent with the following tectonic model: (i) Cache Creek ocean basin closure and Cache Creek terrane imbrication and obduction westward over the Stikine terrane between ca. 183 and 172 Ma in the Atlin area; (ii) supracrustal Stikine terrane overlies an established crustal reservoir of arc character and is not part of a klippe overlying a thick package of Paleozoic or Proterozoic continental margin rocks; (iii) the western Cache Creek terrane structurally overlies the Stikine terrane, and the chemical signatures of plutons that intrude the Cache Creek terrane reflect derivation from the underlying Stikine terrane. Geometric and timing constraints of the new data presented above favour a model for Cache Creek terrane emplacement (Fig. 2d) that is only a slight modification of that proposed by Monger (1977). This interpretation does not favor the megathrust theory advanced by Coney (1989) and others.

Acknowledgments

Aitken, J. D. 1959. Atlin map-area, British Columbia. Geological Survey of Canada, Memoir 307.

Anderson, R. G. 1989. A stratigraphic, plutonic and structural framework for the Iskut map area, northwestern British Columbia. *In* Current research, part E. Geological Survey of Canada, Paper 89-1E, pp. 145−154.

Armstrong, R. L. 1988. Mesozoic and early Cenozoic magmatic evolution of the Canadian Cordillera. *In* Processes in continental lithospheric deformation. *Edited by* S. P. Clark, Jr., B. C. Burchfiel, and J. Suppe. Geological Society of America, Special Paper 218, pp. 55−91.

Ash, C. H., Macdonald, R. W. L., and Arksey, R. L. 1992. Towards a deposit model for ophiolite-related mesothermal gold in British Columbia. *In* Geological fieldwork 1991. British Columbia Ministry of Energy, Mines, and Petroleum Resources, Paper 1992-1, pp. 253−260.

Ballantyne, S. B., and Littlejohn, A. S. 1982. Uranium mineralization and lithogeochemistry of the Surprise Lake batholith, Atlin, British Columbia. *In* Uranium in granites. *Edited by* Y. T. Maurice. Geological Survey of Canada, Paper 81-23, pp. 145−155.

Bloodgood, M. A., and Bellefontaine, K. A. 1990. The geology of the Atlin area (Dixie Lake and Teresa Island) (104 N/6 and parts of 104 N/5 and 12). *In* Geological fieldwork 1989. British Columbia Ministry of Energy, Mines, and Petroleum Resources, Paper 1990-1, pp. 205−216.

Bloodgood, M. A., Rees, C. J., and Lefebure, D. V. 1989. Geology and mineralization of the Atlin area, northwestern British Columbia (104 N/11W and 12E). *In* Geological fieldwork 1988. British Columbia Ministry of Energy, Mines and Petroleum Resources, Paper 1989-1, pp. 311−322.

Bultman, T. R. 1979. Geology and tectonic history of the Whitehorse Trough west of Atlin, British Columbia. Ph.D. thesis, Yale University, New Haven, Conn.

Butler, R. F., Gehrels, G. E., McClelland, W. C., May, S. R., and Klepacki, D. 1989. Discordant paleomagnetic poles from the Canadian Coast Plutonic Complex: regional tilt rather than large-scale displacement. Geology, **17**: 691−694.

Christopher, P. A., and Pinsent, R. H. 1982. Geology of the Ruby Creek and Boulder Creek Area near Atlin (104 N/11W). British Columbia Ministry of Energy, Mines, and Petroleum Resources, Preliminary Map 52, scale 1 : 50 000.

Coney, P. J. 1989. Structural aspects of suspect terranes and accretionary tectonics in western North America. Journal of Structural Geology, **11**: 107−125.

Coney, P. J., Jones, D. L., and Monger, J. W. H. 1980. Cordilleran suspect terranes. Nature (London), **188**: 329−333.

Cordey, F., Mortimer, N., Dewever, P., and Monger, J. W. H. 1987. Significance of Jurassic radiolarians from the Cache Creek terrane, British Columbia. Geology, **15**: 1151−1154.

Cordey, F., Gordey, S. P., and Orchard, M. J. 1991. New biostratigraphic data for the northern Cache Creek terrane, Teslin map area, southern Yukon. *In* Current research, part E. Geological Survey of Canada, Paper 91-1E, pp. 67−76.

Currie, L. D. 1992. Metamorphic rocks in the Tagish Lake area, northern Coast Mountains, British Columbia: a possible link between Stikinia and parts of Yukon−Tanana Terrane. *In* Current research, part A. Geological Survey of Canada, Paper 92-1A, pp. 199−208.

Dawson, K. M. 1988. K−Ar age GSC 88-34. *In* Radiogenic age and isotopic studies: report 2. Geological Survey of Canada, Paper 88-2, p. 135.

Donelick, R. A. 1988. Etchable fission track length reduction in apatite: experimental observations, theory and geological applications. Ph.D. thesis, Renesselaer Polytechnic Institute, Troy, N.Y.

Faure, G. 1986. Principles of isotope geology. 2nd ed. John Wiley & Sons, New York.

Gehrels, G. E., McClelland, W. C., Samson, S. D., Patchett, P. J., and Brew, D. A. 1991*a*. U−Pb geochronology of Late Cretaceous and early Tertiary plutons in the northern Coast Mountains batholith. Canadian Journal of Earth Sciences, **28**: 899−911.

Gehrels, G. E., McClelland, W. C., Samson, S. D., and Patchett, P. J. 1991*b*. U−Pb geochronology of detrital zircons from a continental margin assemblage in the northern Coast Mountains, southeastern Alaska. Canadian Journal of Earth Sciences, **28**: 1285−1300.

Gill, J. B. 1981. Orogenic andesites and plate tectonics. Springer-Verlag, Berlin.

Godwin, C. I., Gabites, J. E., and Andrew, A. 1988. Leadtable: a galena lead isotope data base for the Canadian Cordillera, with a guide to its use by explorationists. British Columbia Ministry of Energy, Mines, and Petroleum Resources, Paper 88-4.

Grond, H. C., Churchill, S. J., Armstrong, R. L., Harakal, J. E., and Nixon, G. T. 1984. Late Cretaceous age of the Hutshi, Mount Nansen, and Carmacks groups, southwestern Yukon Territory and northwestern British Columbia. Canadian Journal of Earth Sciences, **21**: 554−558.

Hansen, V. 1990. Yukon−Tanana terrane: a partial acquittal. Geology, **18**: 365−369.

Harland, W. B., Armstrong, R. L., Cox, A. V., Craig, L. E., Smith, A. G., and Smith, D. G. 1990. A geologic time scale 1989. Cambridge University Press, Cambridge.

Harper, G. D. 1984. The Josephine ophiolite, northwestern California. Geological Society of America Bulletin, **95**: 1009−1026.

Harris, N. B. W., Pearce, J. A., and Tindle, A. G. 1984. Geochemical characteristics of collision zone magmatism. *In* Collision tectonics. *Edited by* R. M. Shackleton, A. C. Reis, and M. P. Coward. Geological Society Special Publication (London), no. 19, pp. 67−81.

Hart, C. J. R., and Radloff, J. K. 1990. Geology of the Whitehorse, Alligator Lake, Fenwick Creek, Carcross, and part of Robinson map areas (105 D/11,6,3,2,and 7). Indian and Northern Affairs Canada, Yukon Region, Open File Report 1990-4.

Hildreth, W., and Moorbath, S. 1988. Crustal contributions to arc magmatism in the Andes of central Chile. Contributions to Mineralogy and Petrology, **45**: 445−489.

Irvine, T. N., and Barager, W. R. A. 1971. A guide to the chemical classification of the common volcanic rocks. Canadian Journal of Earth Sciences, **8**: 523−548.

Irving, E., Woodsworth, G. H., Wynne, P. J., and Morrison, A. 1985. Paleomagnetic evidence for displacement from the south of the Coast Plutonic Complex, British Columbia. Canadian Journal of Earth Sciences, **22**: 584−598.

Irving, E., and Wynne, P. J. 1990. Paleomagnetic evidence bearing on the evolution of the Canadian Cordillera. Philosophical Transactions of the Royal Society of London, Series A, **331**: 487−509.

Jackson, J. L., Gehrels, G. E., Patchett, P. J., and Mihalynuk,

M. G. 1991. Stratigraphic and isotopic link between the northern Stikine terrane and an ancient continental margin assemblage, Canadian Cordillera. Geology, 19: 1177–1180.

Kistler, R. W., and Peterman, Z. E. 1978. Reconstruction of crustal blocks of California on the basis of initial strontium isotopic compositions of Mesozoic granitic rocks. United States Geological Survey, Professional Paper 1071.

Krogh, T. E. 1973. A low-contamination method for hydrothermal decomposition of zircon and extraction of U and Pb for isotopic age determinations. Geochimica et Cosmochimica Acta, 37: 485–494.

Krogh, T. E. 1982. Improved accuracy of U–Pb zircon ages by the creation of more concordant systems using an air abrasion technique. Geochimica et Cosmochimica Acta, 46: 637–649.

Ludwig, K. R. 1980. Calculation of uncertainties of U–Pb isotope data. Earth and Planetary Science Letters, 46: 212–220.

Mihalynuk, M. G., and Mountjoy, K. J. 1990. Geology of the Tagish lake area (104 M/8, 9E). In Geological fieldwork 1989. British Columbia Ministry of Energy, Mines, and Petroleum Resources, Paper 1990-1, pp. 181–196.

Mihalynuk, M. G., and Smith, M. T. 1992. Highlights of finalized mapping in the Atlin West map area (NTS 104 N/12W). In Geological fieldwork 1992. British Columbia Ministry of Energy, Mines, and Petroleum Resources, Paper 1992-1, pp. 221–227.

Mihalynuk, M. G., Smith, M. T., Mountjoy, K. J., Nazarchuk, J. N., McMillan, W. J., Ash, C. H., Hammack, J. L., and Dutchak, R. 1992. Geology and geochemistry of the Atlin west (NTS 104 N/12W) map area, British Columbia. British Columbia Ministry of Energy, Mines, and Petroleum Resources, Open-File Map 1992-8.

Monger, J. W. H. 1975. Upper Paleozoic rocks of the Atlin terrane, northwestern British Columbia and south-central Yukon. Geological Survey of Canada, Paper 74-47.

Monger, J. W. H. 1977. Upper Paleozoic rocks of the western Canadian Cordillera and their bearing on Cordilleran evolution. Canadian Journal of Earth Sciences, 14: 1832–1859.

Monger, J. W. H., and Price, R. A. 1979. Geodynamic evolution of the Canadian Cordillera—progress and problems. Canadian Journal of Earth Sciences, 16: 770–791.

Monger, J. W. H., and Ross, C. A. 1971. Distribution of fusulinaceans in the western Canadian Cordillera. Canadian Journal of Earth Sciences, 8: 259–278.

Monger, J. W. H., Price, R. A., and Tempelman-Kluit, D. J. 1982. Tectonic accretion and the origin of the two major metamorphic and plutonic welts in the Canadian Cordillera. Geology, 10: 70–75.

Monger, J. W. H., Wheeler, J. O., Tipper, H. W., Gabrielse, H., Harms, T., Struik, L. C., Campbell, R. B., Dodds, C. J., Gehrels, G. E., and O'Brien, J. 1991. Part B. Cordilleran terranes. Upper Devonian to Middle Jurassic assemblages. In Geology of the Cordilleran Orogen in Canada. Edited by H. Gabrielse and C. J. Yorath. Geological Survey of Canada, Geology of Canada, no 4, pp 281–327.

Morrison, G. W., Godwin, C. I., and Armstrong, R. L. 1979. Interpretation of isotopic ages and $^{87}Sr/^{86}Sr$ initial ratios for plutonic rocks in the Whitehorse map area, Yukon. Canadian Journal of Earth Sciences, 16: 1988–1997.

Mortensen, J. K. 1992. Pre-mid-Mesozoic tectonic evolution of the Yukon–Tanana terrane, Yukon and Alaska. Tectonics, 11: 836–853.

Nunes, P. D. 1980. The Ontario Geological Survey geochronology research program—an overview. In Summary of geochronological studies 1977–1979. Edited by E. G. Pye. Ontario Geological Survey, Miscellaneous Paper 92, pp. 4–6.

Parrish, R. R. 1987. An improved microcapsule for zircon dissolution in U–Pb geochronology. Chemical Geology, 66: 99–102.

Parrish, R. R., and Krogh, T. E. 1987. Synthesis and purification of ^{205}Pb for U–Pb geochronology. Chemical Geology, 66: 103–110.

Pearce, J. A., Harris, N. B. W., and Tindle, A. G. 1984. Trace element discrimination diagrams for the tectonic interpretation of granitic rocks. Journal of Petrology, 25: 956–983.

Roddick, J. C., Loveridge, W. D., and Parrish, R. R. 1987. Precise U/Pb dating of zircon at the sub-nanogram level. Chemical Geology, 66: 111–121.

Samson, S. D., Patchett, P. J., McClelland, W. C., and Gehrels, G. E. 1990. A detailed Nd isotopic investigation of the Taku and Yukon crystalline terranes, SE Alaska: ancient continental margin material between juvenile crust of the Canadian Cordillera. Geological Association of Canada, Program with Abstracts, 15: A117.

Saunders, A. D., and Tarney, J. 1984. Geochemical characteristics of basaltic volcanism within back-arc basins. In Marginal basin geology. Edited by B. P. Kokelaar and M. F. Howells. Blackwell Scientific Publications, London, pp. 59–76.

Spell, T. L., and Norrell, G. T. 1990. The Ropes Creek assemblage: petrology, geochemistry and tectonic setting of an ophiolitic thrust sheet. American Journal of Science, 290: 811–842.

Stacey, J. S., and Kramers, J. D. 1975. Approximation of terrestrial lead isotope evolution by a two-stage model. Earth and Planetary Science Letters, 26: 207–221.

Steiger, R. H., and Jäger, E. 1977. Subcommission of Geochronology: convention on the use of decay constants in geo- and cosmochronology. Earth and Planetary Science Letters, 36: 359–362.

Stevens, R. D., Delabio, R. N., and Lachance, G. R. 1982. Age determinations and geological studies. K–Ar isotopic ages, report 15. Geological Survey of Canada, Paper 81-2.

Taylor, S. R., and McLennan, S. M. 1985. The continental crust: its composition and evolution. Blackwell Scientific Publications Ltd., Oxford.

Tempelman-Kluit, D. J. 1979. Transported cataclastite, ophiolite and granodiorite in Yukon: evidence of arc–continent collision. Geological Survey of Canada, Paper 79-14.

Thorstad, L. E., and Gabrielse, H. 1986. The Upper Triassic Kutcho Formation, Cassiar Mountains, north-central British Columbia. Geological Survey of Canada, Paper 86-16.

Tipper, H. W., Woodsworth, G. J., and Gabrielse, H. 1981. Tectonic assemblage map of the Canadian Cordillera and adjacent parts of the United States of America. Geological Survey of Canada, Map 1505A, scale 1 : 2 000 000.

Wanless, R. K., Stevens, R. D., Lachance, G. R., and Delabio, R. N. 1972. Age determinations and geological studies. K–Ar isotopic ages, report 10. Geological Survey of Canada, Paper 71-2.

Whalen, J. B., Currie, K. L., and Chappell, B. W. 1987. A-type granites: geochemical characteristics, discrimination and petrogenesis. Contributions to Mineralogy and Petrology, 95: 407–419.

Wheeler, J. O., and McFeely, P. 1987. Tectonic assemblage map of the Canadian Cordillera and adjacent portions of the United States of America. Geological Survey of Canada, Open File 1565, scale 1 : 2 000 000.

Wheeler, J. O., Brookfield, A. J., Gabrielse, H., Monger, J. W. H., Tipper, H. W., and Woodsworth, G. J. 1988. Terrane map of the Canadian Cordillera. Geological Survey of Canada, Open File 1894, scale 1 : 2 000 000.

White, A. J. R., and Chappell, B. W. 1983. Granitoid types and their distribution in the Lachlan fold belt, southeastern Australia. In Circum-Pacific plutonic terranes. Edited by J. A. Roddick. Geological Society of America, Memoir 159, pp. 21–34.

White, W. H., Stewart, D. R., and Ganster, M. W. 1976. Adanac (Ruby Creek). In Porphyry deposits of the Canadian Cordillera. Edited by A. Sutherland Brown. Canadian Institute of Mining and Metallurgy, Special Volume 15, pp. 476–483.

York, D. 1967. The best isochron. Earth and Planetary Science Letters, 2: 479–482.

York, D. 1969. Least-squares fitting of a straight line with correlated errors. Earth and Planetary Science Letters, 5: 320–324.

Appendix

TABLE A1. Sample descriptions and locations

Sample no.	Rock type	NTS sheet	Latitude N	Longitude W	Zircon description
Fourth of July batholith					
DVL87-064	Quartz diorite	104 N/13	59°55′30″	133°47′30″	Clear, colourless, euhedral doubly terminated prisms; width:length ($w:l$) = 1:2−4; contain fluid inclusions but no obvious cores, fractions contain many fragments
DVL87-082	Quartz syenite	104 N/12	59°36′23.5″	133°39′44.1″	Clear, colourless, euhedral multifaceted prisms; $w:l$ = 1:1−2; fluid inclusions visible, some grains had a tan stain which was removed by abrasion
Surprise Lake batholith					
DVL87-051	Biotite granite	104 N/11	59°36′10″	133°16′20″	Clear, colourless, doubly terminated prisms; $w:l$ = 1:1−2; fragments; in magnetic fractions 10% of zircons have cloudy cores which were discarded along with metamict zircons
Table Mountain volcanic suite					
NWI89-17-5	Rhyolite − ash-flow tuff	104 M/09	59°40′41″	134°00′56″	Clear, colourless, doubly terminated prisms; $w:l$ = 1:1.5−3; zircons were washed in acid before separation to remove rust